

# Exploring geometric properties of gold nanoparticles using TEM images to explain their chaperone like activity for citrate synthase

Vikas Kaushik<sup>1</sup>, Tapobrata Lahiri<sup>1\*</sup>, Shantiswaroop Singha<sup>2</sup>, Anjan Kumar Dasgupta<sup>2</sup>, Hrishikesh Mishra<sup>1</sup>, Upendra Kumar<sup>3</sup>, Rajeev Kumar<sup>4</sup>

<sup>1</sup>Division of Applied Sciences and Indi-Russian Center for Biotechnology, Indian Institute of Information Technology, Allahabad, India; <sup>2</sup>Department of Biochemistry, University of Calcutta, Calcutta, India; <sup>3</sup>Gautam Buddha Technical University (Formerly U.P. Technical University), Institute of Engineering & Technology Campus, Sitapur Road, Lucknow-226021; <sup>4</sup>Shovit University, Meerut, UP, India; Tapobrata Lahiri – Email: tlahiri@iiita.ac.in; Phone: 91-532-2922242; Fax: 91-532-2430006; \*Corresponding author

Received May 16, 2011; Accepted November 8, 2011; Published December 10, 2011

## Abstract:

Study on geometric properties of nanoparticles and their relation with biomolecular activities, especially protein is quite a new field to explore. This work was carried out towards this direction where images of gold nanoparticles obtained from transmission electron microscopy were processed to extract their size and area profile at different experimental conditions including and excluding a protein, citrate synthase. Since the images were ill-posed, texture of a context-window for each pixel was used as input to a back-propagation network architecture to obtain decision on its membership as nanoparticle. The segmented images were further analysed by k-means clustering to derive geometric properties of individual nanoparticles even from their assembled form. The extracted geometric information was found to be crucial to give a model featuring porous cage like configuration of nanoparticle assembly using which the chaperone like activity of gold nanoparticles can be explained.

## Background:

Nanotechnology deals with the study and manipulation of matter at nanometer scale i.e., in 1-100 nm range [1]. It has been recently used in various fields ranging from electronics, cosmetics, to medicinal applications like targeted drug delivery systems [2, 3, 4, 5]. These applications of nanoparticle have been possible, because of their specific properties that are different from their counterparts at larger scale of size [6]. Nanoparticles of several metals like gold, Iron, and proteins like albumin and gelatin are being increasingly used for medicinal purposes [7, 8, 9]. Among non metallic nanoparticles, albumin nanoparticles are being used for site-directed delivery of antitumor drugs, as these have tendency towards accumulation in solid tumors [8]. Similarly gelatin nanoparticles have been used as immunological adjuvant to elevate both humoral as well as cellular immune responses to antigen [10]. Among metals, gold and iron nanoparticles have been used in traditional ayurvedic

medicines and are being used in modern medicinal interventions [11]. Colloidal gold was successfully used to do the therapy for rheumatoid arthritis in rats [12]. Several studies are under progress to investigate the interaction of gold nanoparticles with proteins. Recently our group has shown presence of anti-glycation property in gold nanoparticles (GNPs) by preventing glycation of eye lens protein  $\alpha$ -crystallin, paving a novel approach for cataract prevention and therapy [13]. In  $\alpha$ -crystallin molecule, amino acids lysine and arginine containing free amino groups are powerful sites for glycation in addition to the N-terminal amino acid. GNPs competitively bind to these free amino groups and N-terminal amino acid and prevent the glycation of these groups. Similarly, study done by Kogan *et al.*, has demonstrated the applicability of GNPs to prevent aggregation of amyloid beta protein and re dissolving the amyloid aggregates [14]. Motivated from these above-referred studies we have chosen to investigate the effect of

GNPs of sizes 20nm and 40 nm to modulate thermal aggregation of an enzymatic protein citrate synthase. The importance of citrate synthase is that it is involved in Kreb's cycle of aerobic respiration. Citrate synthase has optimum activity at room temperature, and even with a slight rise in temperature it starts to lose its activity and gets aggregated [15]. We have studied the interaction of this protein with gold nanoparticles and tried to deduce a reaction-mechanism of this interaction using the concept of pores of GNP assemblies.

## Methodology:

### Experimental

#### Synthesis of gold nanoparticles:

Gold nanoparticle of different size was synthesized by chemical reduction method as describe by Storhoff *et al.* [16]. Here gold (III) salt like chloro auric acid ( $\text{HAuCl}_4$ ) (0.256 mM) was reduced by tri-sodium citrate (0.52mM) for preparation of smaller nanoparticles and for larger nanoparticle particle we used less amount of reducing agent (0.15 mM) keeping the auric chloride concentration same .

#### Interaction of gold nanoparticle with protein citrate synthase monitored by TEM:

Citrate synthase (0.0032mg/ml) was incubated with two different types of gold nanoparticle for 1 hour at 45°C. The TEM images were taken for both particle at 0min and 60 min of the reaction as described by Singha *et al.* [15]. These TEM (FEI, Czech Republic, type FP 5018/40 TECHNAI G2 SPIRIT BioTWIN) images are used for computational analysis to explain the possible mechanism for prevention of protein heat aggregation by gold nanoparticle.

### Computational

#### Preprocessing and segmentation of images:

Each image was converted to gray scale and resized to 1/3rd of the original size to ease further processing. Part of images representing nanoparticles were segmented out from background using an artificial neural network based texture-segmentation protocol. In this protocol each pixel was defined by its context window (CW) surrounding it the size of which was fixed as 9x9. CW texture defined by the intensities of its pixels was fed as input to the ANN to yield a (1, -1) output for object (-1, 1) output for background. Finally the object and background pixel values were assigned as 1 and 0 respectively. The training data points (i.e., pixels) were carefully chosen to include all variety of contexts of types, i) points within the object, ii) points near the edge but inside the objects, iii) points at the border of the objects, iv) points near the edge but outside the objects, v) points near or at the edge of the image frame. Moreover the training data points were selected from all the image types as described in image acquisition section. CW texture information for 120 pixels from nanoparticle area and background area of images were captured, out of which 84 CWs were used as training input data, and remaining 36 for testing. The ANN we used for this purpose was a four layered feed-forward backpropagation network having 81, 42, 21, and 2 neurons in input, first hidden, second hidden, and output layer respectively.

#### Clustering of object-pixels to isolate individual nanoparticles in segmented images:

Pixels representing nanoparticles were clustered, using k-means clustering to arrange the pixels representing different nanoparticles into separate groups. Value of k was manually counted by observing images having different number of GNPs. In the clustering protocol the initial cluster centres were chosen by clicking mouse at nearly the GNP-centres to avoid early and erroneous convergence of clustering process. The clusters actually represented individual GNP and from the pixels within it we calculated size of each GNP presented within the respective image. Size of a GNP was calculated using its diameter in pixel unit where its radius was calculated as the distance of the maximally distant point from the cluster centre. The area of GNP was however calculated by counting the total pixels covering it. Finally size and area units were converted to nm and  $\text{nm}^2$  respectively by using scale given in right-bottom corner of each image as shown by Singha *et al.* [15]. Arithmetic mean, median, and standard deviation for these geometric features was calculated for each group of images. These measures were compared for evaluating the effect of interaction of nanoparticles and citrate synthase (CS).

#### Computation of expected area and size of pores of clusters made by circular objects:

For rough estimation of size and area of pores of GNP clusters, we considered GNPs as spherical objects and their 2D projection as circles. Initially 2D pore-area covered by these circles was computed to finally estimate the size of these pores. Since visual representation of GNP40 clusters shows a major existence of pores made by 3-circle compact cluster conformation with occasional presence of that made by 4 circles and the reverse situation for GNP20, we computed the size parameters for these examples only. Expected pore area made by 3 and 4-circle compact cluster conformation (as shown in **Figure 1e**) for circle of radius, R as shown in **supplementary material**

#### Computation of size of protein citrate synthase:

The PDB structure of citrate synthase with PDB code, 1CSC.pdb was first downloaded and then read through MATLAB library function `pdbread`. From the coordinates of the atoms of this protein, its centroid and maximum radius (i.e., distance of maximally distant atom from centroid) was calculated. Finally size of the protein was estimated as its diameter.

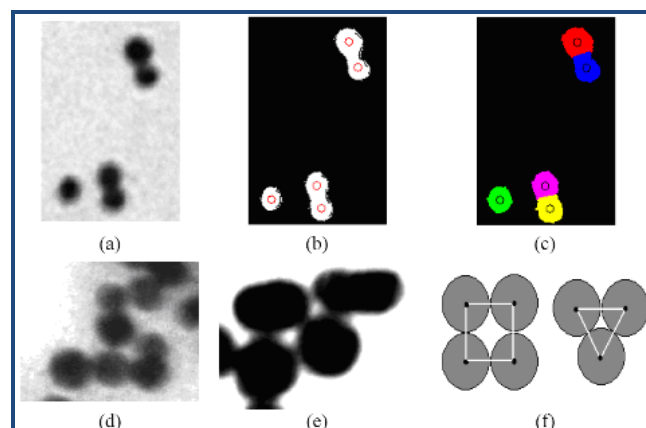


**Figure 1:** Result of a) image of GNP of size 20 nm at 0 min of the reaction with protein; b) their segmented form and c) their individual form; d) and e) GNP20 and GNP40 clusters

respectively in presence of citrate synthase; f) diagram developed from cluster pore theoretics for 3 and 4 circular objects.

## Results and discussion:

Result of image processing was shown for GNP20 as shown in **Figure 1 (a), (b) and (c)**. Diameter of citrate synthase with PDB code, 1CSC.pdb was calculated as 8.23 nm. The image processing task was performed with primarily three objectives. First was to estimate geometric profiles of individual GNPs that might have significance in giving insight to whether chaperone like activity of GNP has any dependence on its surface. To find individual geometric profile of GNP we relied on k-means clustering technique [17] by manually counting and selecting the cluster number and cluster centres respectively. **Figure 1 a-c** showed significant success in achieving this goal. (**Table 1 see supplementary materials**) showed that average size of GNP20 and GNP40 in presence of protein were 24.74 and 48.02 nm respectively. The second objective was to study whether chaperone like activity of GNP was dependent on total surface area of GNPs present in a particular experimental condition. Starting with the existing knowledge [15] that GNP-constituent gold atom is constant we get the indication that number and total surface area of GNP40s present in the solution is less than GNP20. Therefore we found that reported [15] less increase of protein activity exhibited by GNP20 in comparison to GNP40 in the reported experimental condition cannot be interpreted as positive dependence of chaperone activity of GNP with total GNP surface. Thus it also cross-validated the earlier reported findings. Our third objective was to study the effect of size profiles of both GNPs and the porous configurations within their clusters to control protein activity and aggregation. Table 1 showed more increase of average size of GNP20 (30.21%) in comparison to GNP40 (15.2%) in presence of protein. To explain the underlying cause of this increase in size of GNPs we also calculated the expected pore size profiles at different size of GNPs considering them as spheres. It was intriguing to observe that pores obtained by compact 4 circle cluster configuration made by circle of size (i.e., diameter) 20 can just accommodate a single protein of size 8.23 nm (as shown in result section) while its compact 3 circle compact circle counterpart cannot accommodate even a single protein. The image of GNP20 clusters [15] also supported this finding where we get presence of 4 circle cluster configuration is more than other configurations. However, the increase in size of GNP20 within GNP20-clusters in presence of protein appeared to be a reaction mechanism favoring entry of protein molecules within its porous configuration by enhancing its pore size. For both of 3 and 4 circle porous configurations made by GNP40 the pore size was already found to be fit to accommodate single protein molecules and therefore, increase in size of GNP40 was not needed to be that much favored by the same reaction mechanism. Therefore, the reaction mechanism driving increase of GNP-size in presence of protein appears to be controlled by the need of accommodating protein molecules within the porous configurations made by their clusters. It also indicated existence of an optimum size of GNP for cellular interaction is

40 to 60 nm [18]. Finally it appeared that porous configurations of GNP clusters were responsible to give its chaperone like activity by accommodating single protein molecules within it to retain their activity and thus by preventing its aggregation. Also, pores appeared to have an optimum size range, possibly to accommodate single protein molecules only, more than which may lead to formation of protein aggregates within pore, and thereby reducing citrate synthase activity.

## Conclusion:

An image processing based geometric theoretic approach was presented as an experiment support system to compliment investigation of nanoparticle driven biological phenomena. This introductory approach showed its effectiveness by extracting size information of nanoparticles and porous configurations of their clusters. It also indicated the possible role of GNP geometry to show its chaperone like activity by retaining citrate synthase activity in an experimental condition that should favor its aggregation. Our study also showed a possible existence of a model describing this role where porous configuration of GNPs of an optimum size or a range of size accommodating single protein was appeared to serve a role both to prevent protein aggregation and to retain its activity.

## Acknowledgment:

We are thankful to MHRD, Govt. of India and ICMR, Govt. of India for approval of grants (No.F.26-14/2003.T.S.V.Dated 14.01.2004 and No. 52/8/2005-BMS, dated 4/2/10) for this work.

## References:

- [1] El-Ansary A & Al-Daihan S, *J Toxicol* 2009 **2009**: 754810 [PMID: 20130771]
- [2] Kreuter J *et al. Adv Drug Deliv Rev.* 2001 **47**: 65 [PMID: 11251246]
- [3] Deng L *et al. Anal Chem.* 2010 **82**: 4283 [PMID: 20402491]
- [4] Soppimath KS *et al. J Control Release.* 2001 **70**: 1 [PMID: 11166403]
- [5] Choksi AN *et al. J Drugs Dermatol.* 2010 **9**: 475 [PMID: 20480790]
- [6] Kim J *et al. Acta Biomater.* 2010 **6**: 2681 [PMID: 20083240]
- [7] Petrelli F *et al. Expert Opin Pharmacother.* 2010 **11**: 1413 [PMID: 20446855]
- [8] Takakura Y *et al. Pharm Res.* 1990 **7**: 339 [PMID: 1694582]
- [9] Liu G *et al. Methods Mol Biol.* 2010 **610**: 123 [PMID: 20013176]
- [10] Nakaoka R *et al. Vaccine.* 1995 **13**: 653 [PMID: 7545344]
- [11] Bajaj S *et al. Indian J Med Res.* 2001 **113**: 192 [PMID: 11968954]
- [12] Jaeger GT *et al. Acta Vet Scand.* 2007 **49**: 9 [PMID: 17381835]
- [13] Singha S *et al. Nanomedicine.* 2009 **5**: 21 [PMID: 18676206]
- [14] Kogan MJ *et al. Nano Lett* 2006 **6**: 110 [PMID: 16402797]
- [15] Singha S *et al. J Nanosci Nanotechnol.* 2010 **10**: 826 [PMID: 20352724]
- [16] Storhoff JJ *et al. J Am Chem Soc.* 1998 **120**: 1959.
- [17] Lloyd SP. *IEEE Trans Inform Theory* 1982 **IT-28**: 129.
- [18] Jiang W *et al. Nat Nanotechnol* 2008 **3**: 145 [PMID: 18654486]

Edited by P Kanguane

Citation: Kaushik *et al.* Bioinformation 7(7): 320-323 (2011)

**License statement:** This is an open-access article, which permits unrestricted use, distribution, and reproduction in any medium, for non-commercial purposes, provided the original author and source are credited.

## Supplementary material:

Circle of radius R is:

$$E_R(3) = \left[ 2 \sin\left(\frac{\pi}{3}\right) - \frac{\pi}{3} \right] R^2 = 0.1613 \times R^2, \text{ and } E_R(4) = [4 - \pi] R^2 = 0.8584 \times R^2 \text{ respectively.}$$

Corresponding sizes of the pores made by n-circle compact clusters was computed as:

$$S_R(n) = \sqrt{E_R(n)}$$

**Table 1:** Average size and area statistics of GNP at various conditions. P+ and P- represent experiments with and without protein.  $S_R(n)$  and  $S_R(n)$  represent expected pore size made by n circles considering a radius of R of GNP20 and GNP40 as circles of diameter 20 and 40 nm respectively

		Radius	Area	$S_R(3)$	$S_R(4)$
GNP20	P-	9.50 ± 1.18	212.18 ± 61.57	4.02	9.27
	P+	12.37 ± 1.59	319.85 ± 60.21		
GNP40	P-	20.85 ± 1.81	1007.58 ± 152.11	8.03	18.53
	P+	24.02 ± 1.52	1172.65 ± 148.32		